



**HAL**  
open science

# Doubly Base-Stabilized Diborane(4) and Borato-Boronium Species and Their Chemistry with Chalcogens

Asif Ahmad, Sourav Gayen, Shivankan Mishra, Zeenat Afsan, Sébastien Bontemps, Sundargopal Ghosh

► **To cite this version:**

Asif Ahmad, Sourav Gayen, Shivankan Mishra, Zeenat Afsan, Sébastien Bontemps, et al.. Doubly Base-Stabilized Diborane(4) and Borato-Boronium Species and Their Chemistry with Chalcogens. *Inorganic Chemistry*, 2024, 63 (7), pp.3376-3382. 10.1021/acs.inorgchem.3c03961 . hal-04633025

**HAL Id: hal-04633025**

**<https://hal.science/hal-04633025v1>**

Submitted on 3 Jul 2024

**HAL** is a multi-disciplinary open access archive for the deposit and dissemination of scientific research documents, whether they are published or not. The documents may come from teaching and research institutions in France or abroad, or from public or private research centers.

L'archive ouverte pluridisciplinaire **HAL**, est destinée au dépôt et à la diffusion de documents scientifiques de niveau recherche, publiés ou non, émanant des établissements d'enseignement et de recherche français ou étrangers, des laboratoires publics ou privés.

# Doubly Base-Stabilized Diborane(4) and Borato-Boronium Species and Their Chemistry with Chalcogens

*Asif Ahmad,<sup>1</sup> Sourav Gayen,<sup>1</sup> Shivankan Mishra,<sup>1</sup> Zeenat Afsan,<sup>1</sup> Sébastien Bontemps,<sup>2</sup> and Sundargopal Ghosh<sup>\*1</sup>*

<sup>1</sup> Department of Chemistry, Indian Institute of Technology Madras, Chennai 600036, India. Tel: +91 44-22574230; Fax: +91 44-22574202; E-mail: [sghosh@iitm.ac.in](mailto:sghosh@iitm.ac.in)

<sup>2</sup> LCC-CNRS, Université de Toulouse, CNRS, 205 route de Narbonne, 31077 Toulouse Cedex 04, France. E-mail: [sebastien.bontemps@lcc-toulouse.fr](mailto:sebastien.bontemps@lcc-toulouse.fr)

KEYWORDS: diborane, borato-boronium, oxidative insertion, chalcogenido.

## ABSTRACT

In an effort to isolate diborane(4) derivatives, we have developed an efficient and un-catalyzed approach using [BH<sub>3</sub>.THF] and mercaptopyridine ligand. Thermolysis of 2-mercaptopyridine, in presence of [BH<sub>3</sub>.THF] afforded a doubly-base stabilized diborane(4) species **1**, [HB( $\mu$ -C<sub>5</sub>H<sub>4</sub>NS)]<sub>2</sub> along with the formation of its isomeric species **2**, [HB( $\mu$ -C<sub>5</sub>H<sub>4</sub>NS)]<sub>2</sub>, albeit in less yield. Based on the coordination of the boron with mercaptopyridine ligand in **2** and its spectroscopic data, compound **2** has been designated as borato-boronium species, in which the anionic borate and cationic boronium units are covalently bonded to each other. Further, we have demonstrated the oxidative insertion of chalcogen atoms (S and Se) into the B-B bond of the base-stabilized diborane(4), **1** that yielded chalcogenido-diboron species, **3**(S) and **4**(Se).

## INTRODUCTION

Considerable chemistry of boron, particularly in the field of diborane chemistry, is developed by mimicking carbon, offsetting the inherent electron deficiency of boron.<sup>1</sup> In this context, two important strategies, for example, Lewis donor ligands and transition metal templates led to the stabilization of various boron analogues of alkanes, alkenes, alkynes, etc.<sup>2</sup> Although the synthesis and chemistry of diborane(4) has emerged as a new field owing to its wide range of applications, such as borylation reactions, catalytic diboration and natural product synthesis,<sup>3,4</sup> only a handful of diborane compounds are commercially available. As a result, many groups around the world got involved in the synthesis of electron-precise diborane(4) compounds. For example, Cheng *et al.* isolated diborane(4) from the irradiation of diborane(6) with far-UV light.<sup>5</sup> As shown in Chart 1, Himmel and co-workers synthesized a diborane(4), **I** from the dimerization and repeated H<sub>2</sub> elimination of a new guanidine-borane compound.<sup>6</sup> Further, Wagner and co-workers structurally

isolated a unique triply bridged diborane(4), which is manifested as inorganic [4.3.3]propellane with a central B-B bond, **II**.<sup>7</sup> Recently, Fontaine *et al.* reported an unusual B-H activation of FLP moiety in hydroborane that led to B-B dehydrogenative homo-coupling and resulted the diborane(4), **III**.<sup>8</sup> A doubly base-stabilized diborane, **IV** was synthesized from the one electron reduction and subsequent dimerization of borenium cationic salt.<sup>9</sup> Nielsen and Skrydstrup isolated a  $sp^3$ - $sp^3$  diborane(4) species  $[(C_4H_9NO_2B)_2]$  from the reaction of dihydroxyboron with diethanolamine.<sup>10</sup> Although recent years witnessed a widespread increase in the utilization of  $sp^3$ - $sp^3$  diboron(4) reagents, very few synthetic strategies are testified in literature.<sup>1b</sup> Typically, strong reducing conditions and metal-catalyzed dehydrogenative coupling are employed as synthetic tools.<sup>1d-g</sup>

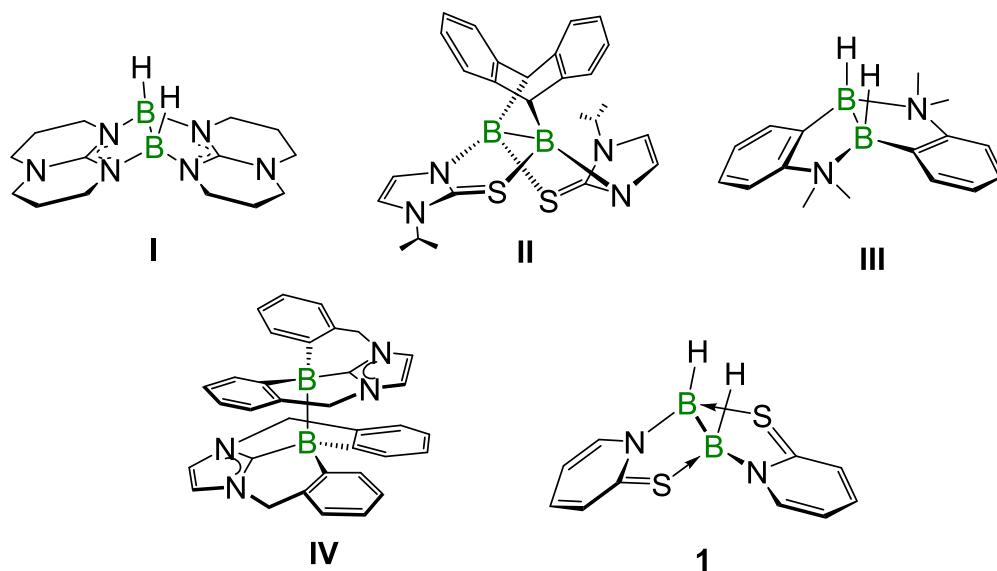


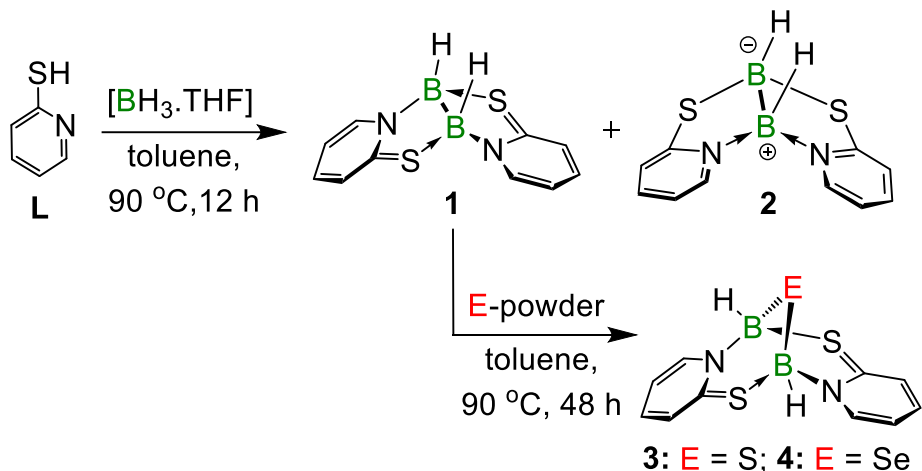
**Chart 1.** Examples of various diborane species **I-IV** and **1**.

While several groups have extended their research on synthesis of diborane starting from various organoboranes, haloboranes as well as hydroboranes,<sup>1b</sup> we have isolated a series of classical and non-classical diborane(4) and diborane(6) stabilized in the coordination sphere of

transition metals (TM).<sup>2a,2e-f,11</sup> In this context, a neutral diborane(6) was isolated from the reaction of diruthenium analogue of pentaborane(9) with 2-mercaptobenzothiazole.<sup>11a</sup> Nevertheless, the complexation of various diborane species with transition metal scaffolds are less investigated. With an objective of exploring the interaction of B-H and B-B bond of diboranes with TM-templates, we sought to synthesize new diborane species and examine their reactivity with metals. Herein, we report the synthesis, structure and bonding of a doubly-base stabilized diborane(4), **1** and an unprecedented borato-boronium species, **2** that shows unique electronic features. Further, the chemistry of both these species with chalcogen atoms has been explored.

## RESULTS AND DISCUSSION

**Syntheses of diborane(4) and borato-boronium species.** As a result, we have carried out the reaction of mercaptopyridine, **L** with [BH<sub>3</sub>·THF] at elevated temperature that yielded compound **1** as pale-yellow solid in 41% yield, which was characterized by multinuclear NMR, IR spectroscopy and mass spectrometry. The <sup>11</sup>B{<sup>1</sup>H} chemical shifts at  $\delta = 1.2$  ppm inferred the presence of tetracoordinated boron atom, similar to [HB( $\mu$ -hpp)]<sub>2</sub>,<sup>6</sup> **I** that shows a single <sup>11</sup>B chemical shift at  $\delta = -2.39$  ppm. This <sup>11</sup>B chemical shift is also similar to Wagner's triply bridging diborane(4) comprising hard (N) and soft (S) bounded boron atoms ( $\delta = 6.2$  ppm).<sup>7b</sup> The <sup>1</sup>H NMR spectrum revealed typical aromatic region peaks as well as peak at  $\delta = 3.9$  ppm due to the presence of B-H<sub>t</sub>. The ESI-MS spectrum revealed the isotopic distribution patterns at  $m/z$  243.0312 consistent with [C<sub>10</sub>H<sub>9</sub>B<sub>2</sub>N<sub>2</sub>S<sub>2</sub>]<sup>+</sup>. Based on all the spectroscopic data along with the mass spectrometric data it is reasonable to assume **1** as diborane(4) species. To validate the spectroscopic data and to determine the solid-state X-ray structure of **1**, single crystal X-ray diffraction analysis was carried out.



**Scheme 1.** Syntheses and reactivity of diborane, **1** and borato-boronium, **2**.

The solid-state X-ray structure of **1**, shown in Figure 1, distinctly shows the presence of diborane(4) species, in which the bridging mercaptopyridinyl moiety enforces an eclipsed geometry around the B1-B2 bond with a *cis*-arrangement of the H-B-B-H. As a result, the torsional angles, N1-B1-B2-S2 of  $13.03^\circ$  and N2-B2-B1-S1 of  $12.71^\circ$  are meaningfully low that indicates the rigidity of fused system through B-B bond. Although the B-B bond length of  $1.696(4) \text{ \AA}$  is consistent with the B-B single bond, it is shorter as compared to several diborane(4) species listed in Chart 1; e.g.;  $[HB(\mu\text{-hpp})]_2$ ,<sup>6b</sup> **I** ( $1.772(3) \text{ \AA}$ ),  $[1\text{-NMe}_2\text{-2-(BH)C}_6\text{H}_4]_2$ ,<sup>8</sup> **III** ( $1.740(2) \text{ \AA}$ ) and Wagner's triply bridging diborane,<sup>7b</sup> **II** ( $1.734(3) \text{ \AA}$ ). The B-N ( $1.600(3) \text{ \AA}$ ) and the B-S ( $1.940(3) \text{ \AA}$ ) bond distances are in good agreement with **II**. The DFT optimized structure of **1** shows an abruptly high H-B-B angle of  $123.8^\circ$  that evidently suggests a greater *s*-character on the boron centres, which may be due to the incidence of B←S Lewis acid-base adduct. This was further confirmed by natural charge distribution obtained from NBO analysis. All these experimental as well as theoretical data suggest **1** as a doubly base stabilised diborane(4) species.

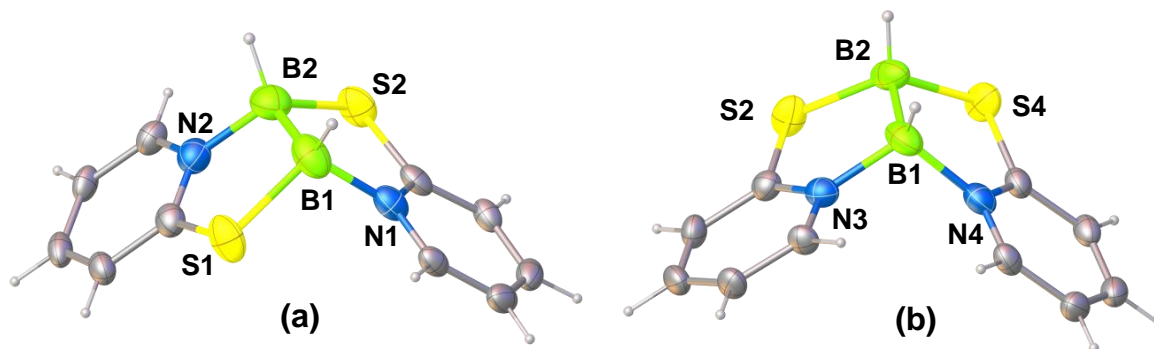


**Figure 1.** Molecular structures of **1**(a) and **2**(b). Selected bond lengths (Å) and angles (°): **1** (a) B1–B2 1.696(4), B1–N1 1.600(3), B1–S1 1.940(3), S1–B1–B2 103.20(18); **2** (b) B1–B2 1.728(10), S2–B2 1.930(9), S4–B2 1.938(7), N3–B1 1.589(7), N4–B1 1.616(8), N3–B1–N4 108.3(4).

Along with the formation of diborane(4) species **1**, we have also isolated **2**, albeit in lower yield. The  $^1\text{H}$  NMR shows the peaks in the range of  $\delta = 8.34\text{--}6.93$  ppm for mercaptopyridinyl moiety. The  $^{11}\text{B}\{^1\text{H}\}$  NMR shows two peaks at  $\delta = 12.4$  and  $-9.5$  ppm suggesting two distinct boron environments. In addition, the  $^1\text{H}$  NMR spectrum shows two broad peaks at  $\delta = 4.34$  and  $3.43$  ppm that correspond to  $\text{BH}_i$ . The mass spectrometric data shows a peak at  $m/z$  243.0304, similar to the corresponding  $[\text{M-H}]^+$  peak of **1**. Although, the combined spectroscopic and ESI-MS data implicitly imply the formation of unsymmetrical diboron species, a precise explanation could not be envisaged until the single-crystal X-ray diffraction study was performed. The solid-state X-ray structure of **2** distinctly shows two mercaptopyridinyl rings that adopt a vicinal configuration along the B-B bond, similar to that of **1**. However, one of the boron atoms (B2) is bonded to two mercaptopyridinyl sulfur atoms (S2 and S4), while the nitrogen atoms (N3 and N4) are connected to B1. As a result, two boron centers in **2** have two distinct coordination modes, in which B1 has two coordinated B-N bonds and two S atoms are covalently bonded to B2. In addition, the B-B bond length of 1.728(10) Å is slightly elongated as compared to **1**.

**Table 1.** Calculated bonding parameters of compounds **1** and **2**.

	Bond length (Å)			Natural Charge (q)		
	$d_{[B-B]}$	$d_{[B-N]}$	$d_{[B-S]}$	$q_B$	$q_N$	$q_S$
<b>1</b>	1.726	1.595	1.977 1.978	-0.103 (B1,B2)	-0.426	0.127
<b>2</b>	1.728	1.622 1.599	1.948 1.922	-0.409(B2) 0.178(B1)	-0.441 -0.439	0.173 0.186

Density Functional Theory (DFT) was carried out to get an insight on the bonding of **2**. The HOMOs of **1** and **2** show B-B  $\sigma$ -bonding interactions along with the presence of non-bonding orbitals on S-atoms (Figure 2). On the other hand, the LUMOs show a delocalization of  $\pi$ -type orbitals over mercaptopyridinyl ring system. Further, on moving from **1** to **2**, the HOMO is getting destabilised along with the stabilization of LUMO, which reduces the HOMO-LUMO energy gap of **2**. The calculated parameters associated with the B-B bond in **2** shows close resemblance with **1** signifying the covalent nature of the B-B bond. Also, the NBO analysis proposes non-equivalent type of boron in **2**. While, the boron atoms in **1** possess similar charge accumulation, an unequal charge distribution was observed in **2** (Table 1). As a result, this generated electron-rich B2 and electron-deficient B1 centers in **2**. Note that recently Jemmis proposed  $[(PH_3)_2B_2Br_2]$  as boryl-borylene species in which a large donor–acceptor contribution was observed from  $P_2B$  unit to the  $BBR_2$  boron.<sup>12</sup> Later, Braunschweig and co-workers isolated a borylene-borane type of adduct,  $[BrB_2PMe_3(\mu-C_7H_6PCy_2)(Bcat)_2]$  from the 1,2-diboration of boryl-borylene,  $[BrB_2PMe_3(\mu-C_7H_6PCy_2)]$ .<sup>13</sup> However, the covalent nature of the B-B bond ruled out the possibility of describing **2** as borylene-borane type of species.



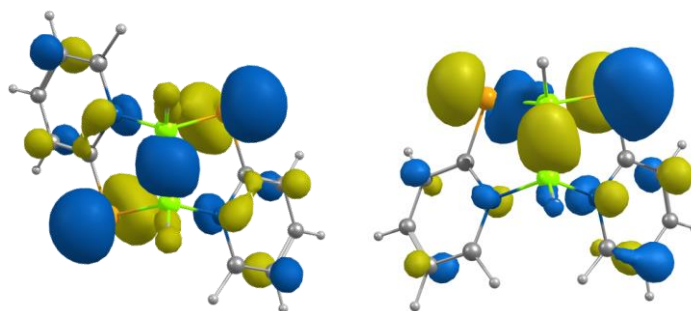
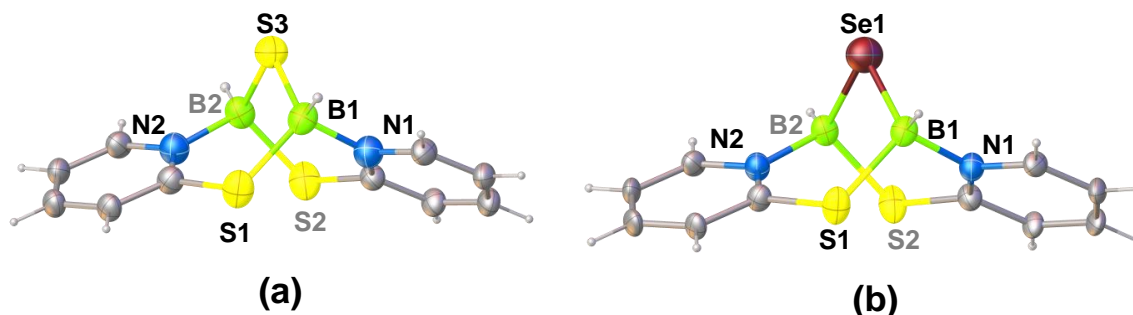


**Figure 2.** HOMOs of **1** (left) and **2** (right).

Therefore, based on the comparative bonding analysis, presence of two diverse  $^{11}\text{B}$  chemical shifts, and the theoretical studies, shown in Figure 2, Tables 1, and S1, compound **2** can best be explained as borato-boronium species. Note that, the structural features of **2** are similar to that of diphenylboronium dimethyl-bis(2-pyridyl)borate.<sup>14</sup> Based on some known borate and boronium species,<sup>15,16</sup> the  $^{11}\text{B}$  chemical shift at  $\delta = -9.5$  has been assigned to the negatively charged borate boron and the peak at 12.4 ppm has been assigned to the positively charged boronium boron (Scheme 1).

**Oxidative addition of chalcogens (S, Se).** To explore the nucleophilicity of the boron centers, we have reacted **1** with sulfur (Scheme 1). The reaction generated a pale yellow solid **3** in 37% yield, which was characterized by multinuclear NMR, IR spectroscopy and mass spectrometry. The  $^{11}\text{B}\{^1\text{H}\}$  NMR spectrum of **3** shows the presence of single boron environment at  $\delta = -4.7$  ppm. The  $^1\text{H}$  NMR spectrum shows the characteristic  $^1\text{H}$  chemical shifts for mercaptopyridine ligand in the region  $\delta = 8.39\text{-}7.03$  ppm. Mass spectrometric data showed an intense ion peak (ESI<sup>+</sup>) at  $m/z$  277.0286, consistent with the molecular formula of  $\text{C}_{10}\text{H}_{11}\text{B}_2\text{N}_2\text{S}_3$ . The single crystal X-ray diffraction analysis was carried out on suitable crystal of **3** to validate the structure of **3**. The molecular structure of **3**, shown in Figure 3, indeed shows that an oxidative insertion of sulfur into the B-B bond led to the formation of bicyclo-[3.3.1]-(sulfido) diboron, **3** in which both of the boron

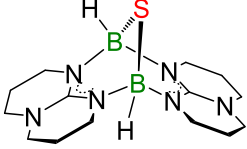
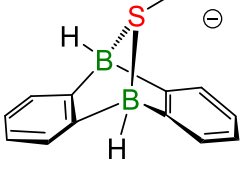
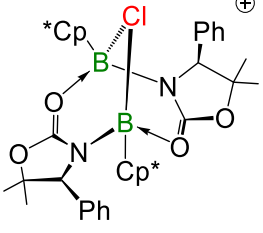
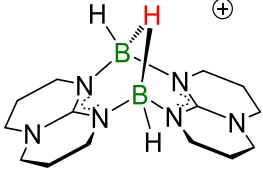
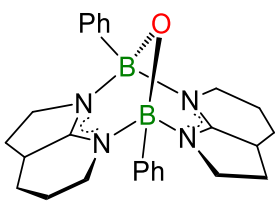
atoms are in +3 oxidation state. Note that, compound **2**, featuring two electronically different boron centers, does not undergo oxidative insertion of S into B-B bond.



**Figure 3.** Molecular structures of **3** (a) and **4** (b). Selected bond lengths (Å) and angles (°): **3** (a) S1–B1 1.940(3), S3–B1 1.865(3), N1–B1 1.580(3), B1–S3–B2 94.35(17), S1–B1–N2 108.45(18); **4** (b) S1–B1 1.929(5), Se1–B1 1.999(4), N1–B1 1.582(6), B1–Se1–B2 89.9(2), S1–B1–N1 109.0(2).

The solid-state X-ray structure of **3** features a [3.3.1]-bicyclic structure, where two tetracoordinated boron atoms are placed at the bridgehead position (Figure 3a). Both the B atoms are connected through N and S atoms with S3–B1–S1 bond angle of 113.6° and B1–S3 bond length of 1.865 Å. They are comparable with the N–B–N bond angles of 109.7° and 110.7° and B–S bond lengths of 1.866(2) Å and 1.894(2) Å observed in [HB( $\mu$ -hpp)]<sub>2</sub>( $\mu$ -S), **V**.<sup>17</sup> In contrast, the chalcogenide bridged organoborane,<sup>7b</sup> {[H<sub>3</sub>CB( $\mu$ -C<sub>6</sub>H<sub>4</sub>)]<sub>2</sub>( $\mu$ -SCH<sub>3</sub>)]<sup>2-</sup>]<sub>2</sub>Li<sup>+</sup>, **VI** shows longer B–S bond lengths (2.089(6) Å, and 2.072(5) Å) and comparable C–B–C bond angles (109.4°, and 110.1°). The B···B separation of 2.736 Å in **3** is significantly longer as compared to several chalcogen and halogen-bridged diboron compounds.<sup>7b,17</sup> However, it is significantly shorter than that of oxazolidinone stabilized borenium cation (2.954 Å), {[Cp<sup>\*</sup>B( $\mu$ -oxazol-Ph)]<sub>2</sub>( $\mu$ -Cl)]<sup>+</sup> [Al(OC(CF<sub>3</sub>)<sub>3</sub>)<sub>4</sub>]<sup>-</sup>, **VII**.<sup>18</sup>

**Table 2.** Selected structural parameters and spectroscopic data of various bicycle organoborane species.

Organoborane	$\angle\text{L-B-L}'(^{\circ})^a$	$d_{[\text{B}\dots\text{B}]}(\text{\AA})$	$^{11}\text{B NMR}^b$
 <b>V</b>	110.7(14) 109.7(15)	2.58	-1.9
 <b>VI</b>	109.4(4) 110.1(4)	2.67	4.8
 <b>VII</b>	110.4(9) 110.4(9)	2.95	10.3
 <b>VIII</b>	117.4(2) 116.6(2)	2.22	-2.2
 <b>IX</b>	103.9(4) 104.0(4)	2.46	-42.7

<sup>a</sup> L= N, L'= N (V, VIII, IX); L= C, L'= C (VI); L= N, L'= O (VII); <sup>b</sup> in ppm.

Organoborane species with unique bridging atoms are noteworthy, thus, we have compared the spectroscopic data of **3** with related molecules (Table 2). For example, the sulfur-bridged organoborane species,  $[\text{HB}(\mu\text{-hpp})]_2(\mu\text{-S})$ , **V** was synthesized from the reaction of  $[\text{HB}(\mu\text{-hpp})]_2$ , **I** with  $\text{S}_8$ .<sup>17</sup> The  $^{11}\text{B}$  NMR spectrum of compound **3** is in well agreement with the chalcogen-bridged organoborane ( $\delta = -1.98$  ppm) as well as with protonated doubly base-stabilised diborane

compound  $[\text{HB}(\mu\text{-hpp})]_2(\mu\text{-H})^+\text{I}^-$ , **VIII** ( $\delta = -2.2$  ppm).<sup>6b</sup> Likewise, Wagner's sulfide bridged organoborane species, **VI** shows a similar kind of  $^{11}\text{B}$  chemical shift as that of **3**.<sup>7b</sup> While, the oxo-bridged organoborane,  $[\text{PhB}(\mu\text{-azain})]_2(\mu\text{-O})$ , **IX** made by Wang shows relatively up-field  $^{11}\text{B}$  chemical shift ( $\delta = -42.7$ ) ppm.<sup>[19]</sup> All these results direct that the electron density on boron can be varied by changing the bridging atom as well as the ligand template.

The report on oxidative insertion of heavier chalcogens into B-B bonds of diborane is scarce possibly due to their larger size and orbital mismatch. As a result, we have treated **1** with selenium powder at elevated temperature that resulted in the formation of pale yellow solid **4** in 25% yield. The  $^{11}\text{B}\{^1\text{H}\}$  NMR shows a peak at  $\delta = -6.5$  ppm slightly in the up-field region as compared to **1**. Additionally, the mass spectrometric data showed a molecular ion peak (ESI<sup>+</sup>) at  $m/z$  324.9717, consistent with the molecular formulae of  $[\text{C}_{10}\text{H}_{11}\text{B}_2\text{N}_2\text{S}_2\text{Se}]^+$ . All the spectroscopic data along with mass spectrometric data also suggest oxidative insertion of Se into the B-B bond of diborane **1**. To the best of our knowledge, **4** is the first example of an oxidative selenation into the B-B bond.

The molecular structure of **4**, shown in Figure 3b, can be described as  $[\text{HB}(\mu\text{-C}_5\text{H}_4\text{NS})]_2(\mu\text{-Se})$ , analogous to **3**. The selenium atom bridged symmetrically with two identical B-Se bond lengths of 1.998(4) Å. Although the B-Se-B bond angle of 89.89° is significantly shorter as compared to the B-O-B angle of  $[\text{PhB}(7\text{-azain})]_2(\mu\text{-O})$ ,<sup>19</sup> **IX**, it is essentially comparable with the B-S-B angle in  $[\text{HB}(\mu\text{-hpp})]_2(\mu\text{-S})$ ,<sup>17</sup> **V**. The value of B-Se-B inter orbital angle manifested the use of pure *p*-orbital by bridging Se atom. On the other hand, the B $\cdots$ B separation of 2.824 Å is notably longer than that of lighter chalcogen-bridged organoborane species, listed in Table 2. In contrary, the B $\cdots$ B separation of 2.95 Å in chloride-bridged diboron cation exhibited a higher value as compared to  $[\text{HB}(\mu\text{-C}_5\text{H}_4\text{NS})]_2(\mu\text{-Se})$ , **4** and similar chalcogen-bridged species.<sup>17,19</sup> Thus, we

believe that the steric hindrance due to the presence of heavier Se atom distressed the separation of two boron atoms. The NBO studies of **4** further shows that the oxidative insertion of Se into the B-B bond of **1** developed a sudden increase of electron density on boron atoms unlike **3** (Table S1). As a result, the mercaptopyridinyl sulfur atoms hold higher positive natural charges and the bridging chalcogen atom possesses considerably lower natural charge. This led to concurrent charge transfer from the mercaptopyridinyl sulfur atom to boron and then to the bridging chalcogen atoms (S or Se).

## CONCLUSIONS

In summary, a new method for the isolation of base-stabilized diborane(4) has been established using 2-mercaptopyridine and [BH<sub>3</sub>.THF]. While working on the reaction pathway for the formation of doubly base-stabilized diborane(4), **1**, we have also isolated an unusual borato-boronium species having electron-rich borate and electron-deficient boronium centers. These reactions offered access to two distinct types of molecules; base-stabilized diboron **1** and borato-boronium species **2** through symmetrical and unsymmetrical coordination of 2-mercaptopyridine with two boron atoms. Further, we have demonstrated the oxidative insertion of sulfur and selenium into the B-B bond of diborane(4). Investigation to stabilize base-stabilised diborane(4) and borato-boronium species into the coordination sphere of transition metal templates is currently underway.

## EXPERIMENTAL SECTION

**General procedures and Instrumentation.** All manipulations were conducted by using standard Schlenk line and glove box techniques under an atmosphere of dry argon. Solvents such as toluene, hexane and THF were distilled through Na/benzo-phenoneketyl and dichloromethane

was dried over calcium hydride prior to use under argon. Chloroform-d was degassed by three freeze-thaw cycles, dried over calcium hydride for 12 h, and stored over 4 Å molecular sieves in a Young's ampoule under argon. BH<sub>3</sub>.THF was obtained commercially (Sigma Aldrich) and used as received. The <sup>1</sup>H, <sup>11</sup>B{<sup>1</sup>H}, <sup>13</sup>C{<sup>1</sup>H}, and <sup>31</sup>P{<sup>1</sup>H} NMR spectra were recorded on Bruker 400 and 500 MHz instruments. The residual solvent protons were used as reference (δ, ppm, benzene-d<sub>6</sub>, 7.16, CDCl<sub>3</sub>, 7.26). The <sup>1</sup>H decoupled <sup>11</sup>B{<sup>1</sup>H} spectra of all compounds were processed with a backward linear prediction algorithm to remove the broad <sup>11</sup>B{<sup>1</sup>H} background signal of the NMR tube.<sup>20</sup> The preparative TLC was performed with Merck 105554 TLC silica gel 60 F254 and thickness of layer 250 μm on aluminum sheets with 20x20 cm size. Mass spectra were carried out using Qtof Micro YA263 HRMS instrument and Bruker MicroTOF-II mass spectrometer in ESI ionization mode. UV-vis absorption spectra were gained from Jasco V-650 spectrometer. Infrared spectra were obtained on a Jasco FT/IR-1400 spectrometer.

**Synthesis of 1-2.** In a flame-dried Schlenk tube, 2-mercaptopyridine **L** (500 mg, 0.90 mmol) in 50 mL dry toluene was treated with [BH<sub>3</sub>.THF] at 90° C. The reaction mixture was allowed to stir at 90° C for 12h. The volatile components were removed under vacuum and the remaining residue was extracted into CH<sub>2</sub>Cl<sub>2</sub>/hexane and passed through Celite. After removal of the solvent, the residue was subjected to chromatographic work-up by using TLC plates. Elution with a *n*-hexane/CH<sub>2</sub>Cl<sub>2</sub> (40:60 v/v) mixture yielded pastel yellow solid **1** (223 mg, 41 %) and **2** (65 mg, 12 %).

**1.** *m/z* calculated for [C<sub>10</sub>H<sub>10</sub>B<sub>2</sub>N<sub>2</sub>S<sub>2</sub> - H]<sup>+</sup>: 243.0394, found 243.0312; <sup>11</sup>B{<sup>1</sup>H} NMR (160 MHz, CDCl<sub>3</sub>, 22 °C): δ = 1.2 (br, B); <sup>1</sup>H NMR (500 MHz, CDCl<sub>3</sub>, 22 °C): δ 8.32 (d, J = 6.3 Hz, 2H, Ar<sub>(mp)</sub>), 7.47 (dd, J = 8.0, 7.6 Hz, 2H, Ar<sub>(mp)</sub>), 7.41 (d, J = 8.1, Hz, 2H, Ar<sub>(mp)</sub>), 6.95 (t, J = 6.6 Hz, 2H, Ar<sub>(mp)</sub>), 3.94 (br,d, 2H, B-H<sub>t</sub>); <sup>13</sup>C{<sup>1</sup>H} NMR (125 MHz, CDCl<sub>3</sub>, 22 °C): δ = 171.5 (C=S),

145.7 (C-N), 138.2 ppm ( $Ar_{(mp)}$ ), 125.0 ppm ( $Ar_{(mp)}$ ), 117.9 ppm ( $Ar_{(mp)}$ ); IR ( $CH_2Cl_2$ ):  $\tilde{\nu} = 2421$  (B- $H_t$ ).

2. MS (ESI<sup>+</sup>):  $m/z$  calculated for  $[C_{10}H_{10}B_2N_2S_2 - H]^+$ : 243.0394, found 243.0304;  $^{11}B\{^1H\}$  NMR (160 MHz,  $CDCl_3$ , 22 °C):  $\delta = 12.4, -9.5$  (br, B);  $^1H$  NMR (500 MHz,  $CDCl_3$ , 22 °C):  $\delta$  8.33 (d,  $J = 6.1$  Hz, 2H,  $Ar_{(mp)}$ ), 7.48 (dd, 6.6, 8.5 Hz, 4H,  $Ar_{(mp)}$ ), 6.93 (t,  $J = 6.1$  Hz, 2H,  $Ar_{(mp)}$ ), 4.34, 3.43 (br,d, 2H, B- $H_t$ );  $^{13}C\{^1H\}$  NMR (125 MHz,  $CDCl_3$ , 22 °C):  $\delta = 176.2$  (C=S), 143.8 (C-N), 138.4 ppm ( $Ar_{(mp)}$ ), 126.0 ppm ( $Ar_{(mp)}$ ), 117.3 ppm ( $Ar_{(mp)}$ ); IR ( $CH_2Cl_2$ ):  $\tilde{\nu} = 2426$  (B- $H_t$ ),  $\tilde{\nu} = 2430$  (B- $H_t$ ).

**Synthesis of 3.** In a flame-dried Schlenk tube,  $(C_5H_4NSBH)_2$  **1** (50 mg, 0.18 mmol) in 10 mL dry toluene was treated with S-powder at 90° C. The reaction mixture was allowed to stir at 90° C for 2 days. The volatile components were removed under vacuum and the remaining residue was extracted into  $CH_2Cl_2$ /hexane and passed through Celite. After removal of the solvent, the residue was subjected to chromatographic work-up by using TLC plates. Elution with a *n*-hexane/ $CH_2Cl_2$  (40:60 v/v) mixture yielded pastel yellow solid **3** (21 mg, 37 %).

3.  $m/z$  calculated  $[C_{10}H_{10}B_2N_2S_3 + H]^+$ : 277.0271, found 277.0266;  $^{11}B\{^1H\}$  NMR (160 MHz,  $CDCl_3$ , 22 °C):  $\delta = -4.7$  (br, B);  $^1H$  NMR (500 MHz,  $CDCl_3$ , 22 °C):  $\delta$  8.45 (d,  $J = 6.3$  Hz, 2H,  $Ar_{(mp)}$ ), 7.60 (m,  $J = 7.6, 8.0$  Hz, 4H,  $Ar_{(mp)}$ ), 7.09 (dd,  $J = 6.3, 6.5$  Hz, 2H,  $Ar_{(mp)}$ ), 4.43 (br,q, 2H, B- $H_t$ );  $^{13}C\{^1H\}$  NMR (125 MHz,  $CDCl_3$ , 22 °C):  $\delta = 162.5$  (C=S), 146.8 (C-N), 138.0 ppm ( $Ar_{(mp)}$ ), 130.0 ppm ( $Ar_{(mp)}$ ), 118.4 ppm ( $Ar_{(mp)}$ ); IR ( $CH_2Cl_2$ ):  $\tilde{\nu} = 2432$  (B- $H_t$ ).

**Synthesis of 4.** Under similar reactions conditions, reaction of  $(C_5H_4NSBH)_2$  **1**, (50 mg, 34  $\mu$ mol) was treated with Se-powder. The volatile components were removed under vacuum and the remaining residue was extracted into  $CH_2Cl_2$ /hexane and passed through Celite. After removal of

the solvent, the residue was subjected to chromatographic work-up by using TLC plates. Elution with a *n*-hexane/CH<sub>2</sub>Cl<sub>2</sub> (40:60 v/v) mixture yielded pastel yellow solid **4** (17 mg, 25 %).

**4.** *m/z* calculated for [C<sub>10</sub>H<sub>10</sub>B<sub>2</sub>N<sub>2</sub>S<sub>2</sub>Se + H]<sup>+</sup>: 324.9717, found 324.9542; <sup>11</sup>B{<sup>1</sup>H} NMR (160 MHz, CDCl<sub>3</sub>, 22 °C): δ = -6.5 (*br, B*); <sup>1</sup>H NMR (500 MHz, CDCl<sub>3</sub>, 22 °C): δ 8.52 (*d, J* = 6.1 Hz, 2H, *Ar*<sub>(mp)</sub>), 7.59 (*d, J* = 4.0 Hz, 4H, *Ar*<sub>(mp)</sub>), 7.10 (*dd, J* = 4.8, 5.0 Hz, 2H, *Ar*<sub>(mp)</sub>), 4.62 (*br, q, 2H, B-H<sub>t</sub>*); <sup>13</sup>C{<sup>1</sup>H} NMR (125 MHz, CDCl<sub>3</sub>, 22 °C): δ = 162.8 (C=S), 146.8 (C-N), 137.9 ppm (*Ar*<sub>(mp)</sub>), 130.2 ppm (*Ar*<sub>(mp)</sub>), 118.6 ppm (*Ar*<sub>(mp)</sub>); IR (CH<sub>2</sub>Cl<sub>2</sub>):  $\tilde{\nu}$  = 2417 (B-H<sub>t</sub>).

**X-ray Structure Determination.** Crystal data of **1**, **2** and **4** were collected and integrated using a Bruker AXS Kappa APEXII CCD diffractometer with graphite monochromated Mo K $\alpha$  ( $\lambda$  = 0.71073 Å) radiation at 296(2) K. The crystal data of **3** were collected and integrated using a Bruker D8 VENTURE diffractometer with a PHOTON II detector employing graphite monochromated Mo K $\alpha$  ( $\lambda$  = 0.71073 Å) radiation at 296(2) K. Suitable X-ray quality crystals of **1**, **2**, **3**, and **4** were grown by slow diffusion of a hexane-CH<sub>2</sub>Cl<sub>2</sub> solution at -5 °C. All the structures were solved using SIR92<sup>21</sup> and refined with SHELXL-2018, SHELXL-2014, and SHELXL-2017<sup>22</sup>. Using Olex2<sup>23</sup> all the molecular structures were drawn. The non-hydrogen atoms were refined with anisotropic displacement parameters. All hydrogens could be located in the difference Fourier map. However, the hydrogen atoms bonded to carbons and borons were fixed at chemically meaningful positions and were allowed to ride with the parent atom during the refinement. Crystallographic data have been deposited with the Cambridge Crystallographic Data Center as supplementary publication no CCDC- 2264070 (**1**), CCDC- 2284148 (**2**), CCDC- 2252064 (**3**), CCDC- 2281626 (**4**). These data can be obtained free of charge from The Cambridge Crystallographic Data Centre via [www.ccdc.cam.ac.uk/data\\_request/cif](http://www.ccdc.cam.ac.uk/data_request/cif).



*Crystal data for 1.* C<sub>10</sub>H<sub>10</sub>B<sub>2</sub>N<sub>2</sub>S<sub>2</sub>, M<sub>r</sub> = 243.94, monoclinic, space group *P2<sub>1</sub>/n*, *a* = 6.9543(4) Å, *b* = 25.1365(16) Å, *c* = 7.4615(4) Å, α = 90°, β = 116.947(3)°, γ = 90°, *V* = 1162.71(12) Å<sup>3</sup>, *Z* = 4, ρ<sub>calcd</sub> = 1.394 g/cm<sup>3</sup>, μ = 0.426 mm<sup>-1</sup>, F(000) = 504, *R<sub>I</sub>* = 0.0384, w*R<sub>2</sub>* = 0.0854, 2038 independent reflections [2θ ≤ 49.99°] and 153 parameters.

*Crystal data for 2.* C<sub>10</sub>H<sub>10</sub>B<sub>2</sub>N<sub>2</sub>S<sub>2</sub>, M<sub>r</sub> = 243.94, triclinic, space group *P1*, *a* = 7.0879(7) Å, *b* = 7.2179(7) Å, *c* = 11.9894(12) Å, α = 90.592(5)°, β = 98.861(4)°, γ = 104.352(4)°, *V* = 586.39(10) Å<sup>3</sup>, *Z* = 2, ρ<sub>calcd</sub> = 1.382 g/cm<sup>3</sup>, μ = 0.422 mm<sup>-1</sup>, F(000) = 252, *R<sub>I</sub>* = 0.0479, w*R<sub>2</sub>* = 0.1365, 3492 independent reflections [2θ ≤ 49.99°] and 289 parameters.

*Crystal data for 3.* C<sub>10</sub>H<sub>10</sub>B<sub>2</sub>N<sub>2</sub>S<sub>3</sub>, M<sub>r</sub> = 276.00, monoclinic, space group *C2/c*, *a* = 13.7895(3) Å, *b* = 7.5787(2) Å, *c* = 14.0135(4) Å, α = 90°, β = 119.4030(10)°, γ = 90°, *V* = 1275.86(6) Å<sup>3</sup>, *Z* = 4, ρ<sub>calcd</sub> = 1.437 g/cm<sup>3</sup>, μ = 5.093 mm<sup>-1</sup>, F(000) = 568, *R<sub>I</sub>* = 0.0476, w*R<sub>2</sub>* = 0.1392, 1223 independent reflections [2θ ≤ 67.679 °] and 83 parameters.

*Crystal data for 4.* C<sub>10</sub>H<sub>10</sub>B<sub>2</sub>N<sub>2</sub>S<sub>2</sub>Se, M<sub>r</sub> = 322.90, monoclinic, space group *C2/c*, *a* = 14.0156(11) Å, *b* = 7.4350(6) Å, *c* = 14.2043(16) Å, α = 90°, β = 119.496(3)°, γ = 90°, *V* = 1288.3(2) Å<sup>3</sup>, *Z* = 4, ρ<sub>calcd</sub> = 1.665 g/cm<sup>3</sup>, μ = 3.213 mm<sup>-1</sup>, F(000) = 640, *R<sub>I</sub>* = 0.0313, w*R<sub>2</sub>* = 0.0784, 3426 independent reflections [2θ ≤ 49.99°] and 82 parameters.

**Computational Details.** All the compounds were optimized using the Gaussian 16<sup>24</sup> program. The gradient-corrected B3LYP functional<sup>25</sup> along with def2-tzvp basis set<sup>26</sup> from EMSL7 Basis Set Exchange Library<sup>27</sup> was used for optimization. The model compounds were fully optimized starting from X-ray coordinates in the gaseous state (no solvent effect). Frequency calculations were carried out for the verification of the nature of the stationary state and to confirm the absence of any imaginary frequency which eventually confirmed the minima on the potential energy

hypersurface for all structures. Using the optimized geometries at the B3LYP/def2-TZVP level, NMR chemical shifts were calculated using the gauge-including atomic orbitals (GIAOs) method.<sup>28</sup> The <sup>11</sup>B NMR chemical shifts were calculated relative to B<sub>2</sub>H<sub>6</sub>, with a B3LYP shielding constant of 83.6 ppm. To convert these values to the standard [BF<sub>3</sub>·OEt<sub>2</sub>] scale, the computed values were adjusted by adding 16.6 ppm (the experimental  $\delta$  (<sup>11</sup>B) value of B<sub>2</sub>H<sub>6</sub>). The internal standard used for calculating <sup>1</sup>H NMR chemical shifts was TMS (SiMe<sub>4</sub>). Wiberg bond indices (WBI)<sup>29</sup> was generated from natural bond orbital analysis (NBO)<sup>30</sup>. All the optimized geometries and orbital pictures were drawn by Chemcraft<sup>31</sup> visualization programs. Laplacian electronic distribution plots and two-dimensional electron density were generated using the Multiwfn package.<sup>32</sup>

## **ASSOCIATED CONTENT**

NMR and mass spectra of all complexes, additional DFT results, and optimized coordinates

### **Supporting Information**

The supporting information is available free of charge at via the internet at <http://pubs.acs.org>.

## **AUTHOR INFORMATION**

### **Corresponding Author**

\*E-mail: [sghosh@iitm.ac.in](mailto:sghosh@iitm.ac.in) (S.G.)

### **Author Contributions**

### **Notes**

The authors declare no competing financial interest.

## ACKNOWLEDGMENT

We thankfully acknowledge the support from CSIR (Scheme No. 01(3055)/21/EMR-II), New Delhi, India. A.A and S.G. thanks CSIR, S.M. and Z.A. thanks IITM for research fellowships. We thank Dr. P. K. Sudhadevi Antharjanam, SAIF, IIT Madras and Dr. V. Ramkumar, IIT Madras for X-ray data collection. The computational facility of IIT Madras is gratefully acknowledged.

## NOTES AND REFERENCES

- (a) Légaré, M.-A.; Pranckevicius, C.; Braunschweig, H. Metallomimetic Chemistry of Boron. *Chem. Rev.* **2019**, *119*, 8231–8261; (b) Neeve, E. C.; Geier, S. J.; Mkhaliid, I. A. I.; Westcott, S. A.; Marder, T. B. Diboron(4) Compounds: From Structural Curiosity to Synthetic Workhorse. *Chem. Rev.* **2016**, *116*, 9091–9161; (c) Cuenca, A. B.; Shishido, R.; Ito, H.; Fernández, E. Transition-Metal-Free B–B and B–Interelement Reactions with Organic Molecules. *Chem. Soc. Rev.* **2017**, *46* (2), 415–430; (d) Brotherton, R. J.; McCloskey, A. L.; Petterson, L. L.; Steinberg, H. Tetra-(amino)-diborons. *J. Am. Chem. Soc.* **1960**, *82*, 6242–6245; (e) Shoji, Y.; Matsuo, T.; Hashizume, D.; Gutmann, G. J.; Fueno, H.; Tanaka, K.; Tamao, K. *J. Am. Chem. Soc.* **2011**, *133*, 11058–11061; (f) Wang, Y.; Robinson, G. H. Carbene stabilization of highly reactive main-group molecules. *Inorg. Chem.* **2011**, *50*, 12326–12337; (g) Kim, S.-K.; Han, W.-S.; Kim, T.-J.; Kim, T.-Y.; Nam, S. W.; Mitoraj, M.; Piekoś, Ł.; Michalak, A.; Hwang, S.-J.; Kang, S. O. Palladium Catalysts for Dehydrogenation of Ammonia Borane with Preferential B–H Activation. *J. Am. Chem. Soc.* **2010**, *132*, 9954–9955.
- (a) Saha, K.; Roy, D. K.; Dewhurst, R. D.; Ghosh, S.; Braunschweig, H. Recent advances in the synthesis and reactivity of transition metal  $\sigma$ -borane/borate complexes. *Acc.*

*Chem. Res.* **2021**, *54*, 1260–1273; (b) Litters S., Kaifer E., Enders M. Himmel, H. -J. A boron–boron coupling reaction between two ethyl cation analogues. *Nature Chem.*, **2013**, *5*, 1029–1034; (c) Bamford, K. L.; Qu, Z.-W.; Stephan, D. W. Activation of H<sub>2</sub> and Et<sub>3</sub>SiH by the Borinium Cation [Mes<sub>2</sub>B]<sup>+</sup>: Avenues to Cations [MesB(μ-H)<sub>2</sub>(μ-Mes)BMes]<sup>+</sup> and [H<sub>2</sub>B(μ-H)(μ-Mes)B(μ-Mes)(μ-H)BH<sub>2</sub>]<sup>+</sup>. *J. Am. Chem. Soc.* **2019**, *141*, 6180–6184; (d) Mao, X.; Zhang, J.; Lu, Z.; Xie, Z. A (μ-hydrido)diborane(4) anion and its coordination chemistry with coinage metals. *Chem. Sci.* **2022**, *13*, 3009–3013; (e) Saha, K.; Ghorai, S.; Kar, S.; Saha, S.; Halder, R.; Raghavendra, B.; Jemmis, E. D.; Ghosh, S. Stabilization of Classical [B<sub>2</sub>H<sub>5</sub>]<sup>−</sup>: Structure and Bonding of [(Cp\*Ta)<sub>2</sub>(B<sub>2</sub>H<sub>5</sub>)(μ-H)L<sub>2</sub>] (Cp\* = η<sup>5</sup>-C<sub>5</sub>Me<sub>5</sub>; L = SCH<sub>2</sub>S). *Angew. Chem., Int. Ed.* **2019**, *58*, 17684–17689; (f) Borthakur, R.; Saha, K.; Kar, S.; Ghosh, S. Recent advances in transition metal diborane(6), diborane(4) and diborene(2) chemistry. *Coord. Chem. Rev.* **2019**, *399*, 213021–213037.

3 (a) Kaese, T., Hübner, A., Bolte, M., Lerner, H.-W., Wagner, M., Forming B–B Bonds by the Controlled Reduction of a Tetraaryl-diborane(6). *J. Am. Chem. Soc.* **2016**, *138* (19); (b) Dewhurst, R. D.; Neeve, E. C.; Braunschweig, H.; Marder, T. B. sp<sup>2</sup>-sp<sup>3</sup> diboranes: astounding structural variability and mild sources of nucleophilic boron for organic synthesis. *Chem. Commun.* **2015**, *51*, 9594–9607; (c) Asakawa, H., Lee, K. H., Lin, Z., Yamashita, M., Facile scission of isonitrile carbon–nitrogen triple bond using a diborane(4) reagent. *Nat. Commun.*, **2014**, *5*, 4245; (d) Wagner, A.; Kaifer, E.; Himmel, H.-J. Diborane(4)–metal bonding: between hydrogen bridges and frustrated oxidative addition. *Chem. Commun.* **2012**, *48*, 5277–5279; (e) Thiess, T., Bélanger-Chabot, G., Fantuzzi, F., Michel, M., Ernst, M., Engels, B., Braunschweig, H., Diborane(4) Azides: Surprisingly Stable Sources of Transient Iminoboranes. *Angew. Chem. Int. Ed.*, **2020**, *59*, 15480–15486.

4 (a) Tsukahara, N.; Asakawa, H.; Lee, K.-H.; Lin, Z.; Yamashita, M. Cleaving Dihydrogen with Tetra(o-tolyl)diborane(4). *J. Am. Chem. Soc.* **2017**, *139*, 2593–2596; (b) Mao, X.; Zhang, J.; Lu, Z.; Xie, Z. A ( $\mu$ -hydrido)diborane(4) anion and its coordination chemistry with coinage metals. *Chem. Sci.* **2022**, *13*, 3009–3013; (c) Budy, H., Kaese, T., Bolte, M., Lerner H.-W., Wagner, M., A Chemiluminescent Tetraaryl Diborane(4) Tetraanion. *Angew. Chem. Int. Ed.*, 2021, **60**, 19397–19405; (d) Shoji, Y., Kaneda, S., Fueno, H., Tanaka, K., Tamao, K., Hashizume D., Matsuo, T., An Isolable Diborane(4) Compound with Terminal B–H Bonds: Structural Characteristics and Electronic Properties. *Chem. Lett.*, **2014**, *43*, 1587–1589.

5 Chou, S.-L., Lo, J.-I., Peng, Y.-C., Lin, M.-Y., Lu, H.-C., Cheng B.-M., Ogilvie, J. F., Identification of diborane(4) with bridging B–H–B bonds. *Chem. Sci.*, **2015**, *6*, 6872–6877.

6 (a) Ciobanu, O.; Roquette, P.; Leingang, S.; Wadepohl, H.; Mautz, J.; Himmel, H.-J. Synthesis and Characterization of a New Guanidine–Borane Complex and a Dinuclear Boron(II) Hydride with Bridging Guanidinate Ligands. *Eur. J. Inorg. Chem.* **2007**, 4530–4534; (b) Ciobanu, O.; Kaifer, E.; Enders, M.; Himmel, H.-J. Synthesis of a Stable  $B_2H_5^+$  Analogue by Protonation of a Double Base-Stabilized Diborane(4) *Angew. Chem., Int. Ed.* **2009**, *48*, 5538–5541.

7 (a) Trageser, T., Bebej, D., Bolte, M., Lerner H.-W., Wagner, M., B–B vs. B–H Bond Activation in a ( $\mu$ -Hydrido)diborane(4) Anion upon Cycloaddition with  $CO_2$ , Isocyanates, or Carbodiimides. *Angew. Chem. Int. Ed.*, 2021, **60**, 2–9; (b) von Grotthuss, E.; Nawa, F.; Bolte, M.; Lerner, H.-W.; Wagner, M. Chalcogen-chalcogen-bond activation by an ambiphilic, doubly reduced organoborane. *Tetrahedron* **2019**, *75* (1), 26–30.

8 Rochette, É.; Bouchard, N.; Légaré Lavergne, J.; Matta, C. F.; Fontaine, F.-G. Spontaneous Reduction of a Hydroborane To Generate a B–B Single Bond by the Use of a Lewis Pair. *Angew. Chem., Int. Ed.* **2016**, *55*, 12722–12726.

9 Cao, L. L.; Stephan, D. W. Homolytic Cleavage Reactions of a Neutral Doubly Base Stabilized Diborane(4). *Organometallics* **2017**, *36*, 3163–3170.

10 Flinker, M., Yin, H., Juhl, R. W., Eikeland, E. Z., Overgaard, J., Nielsen D. U., Skrydstrup, T., Efficient Water Reduction with  $sp^3$ - $sp^3$  Diboron(4) Compounds: Application to Hydrogenations, H–D Exchange Reactions, and Carbonyl Reductions. *Angew. Chem. Int. Ed.*, **2017**, *56*, 15910–15915.

11 (a) Anju, R. S.; Roy, D. K.; Mondal, B.; Yuvaraj, K.; Arivazhagan, C.; Saha, K.; Varghese, B.; Ghosh, S. Reactivity of diruthenium and dirhodium analogues of pentaborane(9): agostic versus boratrane complexes. *Angew. Chem., Int. Ed.* **2014**, *53*, 2873–2877; (b) Mondal, B.; Bag, R.; Ghorai, S.; Bakthavachalam, K.; Jemmis, E. D.; Ghosh, S. Synthesis, Structure, Bonding, and Reactivity of Metal Complexes Comprising Diborane(4) and Diborene(2):  $[\{Cp^*Mo(CO)_2\}_2\{\mu-\eta^2:\eta^2-B_2H_4\}]$  and  $[\{Cp^*M(CO)_2\}_2B_2H_2M(CO)_4]$ , M = Mo,W. *Angew. Chem., Int. Ed.* **2018**, *57*, 8079–8083.

12 Ghorai, S.; Jemmis, E. D. A DFT Study on the Stabilization of the B identical with B Triple Bond in a Metallaborocycle: Contrasting Electronic Structures of Boron and Carbon Analogues. *Chem.–Eur. J.* **2017**, *23*, 9746–9751.

13 (a) Stennett, T. E.; Mattock, J. D.; Vollert, I.; Vargas, A.; Braunschweig, H. Unsymmetrical, Cyclic Diborenes and Thermal Rearrangement to a Borylborylene. *Angew. Chem., Int. Ed.* **2018**, *57*, 4098–4102; (b) Stennett, T. E.; Bertermann, R.; Braunschweig, H.

Construction of Linear and Branched Tetraboranes by 1,1- and 1,2-Diboration of Diborenes. *Angew. Chem., Int. Ed.* **2018**, *57*, 15896–15901.

14 Hodgkins, T. G.; Powell, D. R. Derivatives of the Dimethylbis(2-pyridyl)borate(1-) Ion: Synthesis and Structure. *Inorg. Chem.* **1996**, *35*, 2140–2148.

15 Piers, W. E.; Bourke, S. C.; Conroy, K. D. Borinium, borenium, and boronium ions: synthesis reactivity and applications. *Angew. Chem., Int. Ed.* **2005**, *44*, 5016–5036.

16 (a) Dyson, G.; Zech, A.; Rawe, B. W.; Haddow, M. F.; Hamilton, A.; Owen, G. R. Scorpionate Ligands Based on 2-Mercaptopyridine: A Ligand with a Greater Propensity To Sting? *Organometallics* **2011**, *30*, 5844–5850; (b) Owen, G. R.; Hugh Gould, P.; Charmant, J. P. H.; Hamilton, A.; Saithong, S. A new hybrid scorpionate ligand: a study of the metal–boron bond within metallaboratrane complexes. *Dalton Trans.* **2010**, *39*, 392–400; (c) Zafar, M.; Ahmad, A.; Saha, S.; Ramalakshmi, R.; Roisnel, T.; Ghosh, S. Cooperative B-H bond activation: Dual sites borane activation by redox active  $\kappa^2$ -N,S-chelated complexes. *Chem. Sci.* **2022**, *13*, 8567–8575; (d) Zafar, M.; Ramalakshmi, R.; Ahmad, A.; Antharjanam, P. K. S.; Bontemps, S.; Sabo-Etienne, S.; Ghosh, S. Cooperative B-H and Si-H Bond Activations by  $\kappa^2$ -N,S-Chelated Ruthenium Borate Complexes. *Inorg. Chem.* **2021**, *60*, 1183–1194.

17 Schulenberg, N.; Ciobanu, O.; Kaifer, E.; Wadepohl, H.; Himmel, H.-J. The Doubly Base-Stabilized Diborane(4) [HB( $\mu$ -hpp)]<sub>2</sub> (hpp = 1,3,4,6,7,8-hexahydro-2H-pyrimido[1,2-a]pyrimidine): Synthesis by Catalytic Dehydrogenation and Reactions with S<sub>8</sub> and Disulfides. *Eur. J. Inorg. Chem.* **2010**, 5201–5210.

18 Shih, D. -N., Boobalan, R., Liu, Y. -H., Chein R. -J., Chiu, C. -W., [B–Cl–B]<sup>+</sup> Cations: Chloroborane Masked Chiral Borenium Ions. *Inorg. Chem.*, 2021, **60**, 16266–16272.

19 Wu, Q.; Esteghamatian, M.; Hu, N.-X.; Popovic, Z.; Enright, G.; Breeze, S. R.; Wang, S. Isomerism and Blue Electroluminescence of a Novel Organoboron Compound:  $B^{III}_2(O)(7\text{-azain})_2Ph_2$ . *Angew. Chem., Int. Ed.* **1999**, *38*, 985–988.

20 (a) Led, J. J.; Gesmar, H. Application of the Linear Prediction Method to NMR Spectroscopy. *Chem. Rev.* 1991, *91*, 1413–1426. (b) Yang, L.; Simionescua, R.; Lough, A.; Yan, H. Some observations relating to the stability of the BODIPY fluorophore under acidic and basic conditions. *Dyes and Pigments*, **2011**, *91*, 264–267.

21 (a) Sheldrick, G. M. SHELXT - Integrated space-group and crystal-structure determination. *Acta Cryst.* **2015**, *A71*, 3–8. (b) Sheldrick, G. M. SHELXS97 and SHELXL97. Program for Crystal Structure Solution and Refinement, University of Gottingen: Germany, **1997**.

22 Sheldrick, G. M. Crystal Structure Refinement with SHELXL. *Acta Crystallogr., Sect. C: Struct. Chem.* **2015**, *C71*, 3–8.

23 Dolomanov, O. V.; Bourhis, L. J.; Gildea, R. J.; Howard, J. A. K.; Puschmann, H. OLEX2: a complete structure solution, refinement and analysis program. *J. Appl. Crystallogr.* **2009**, *42*, 339–341.

24 Frisch, M. J.; Trucks, G. W., Schlegel, H. B.; Scuseria, G. E.; Robb, M. A.; Cheeseman, J. R. G.; Mennucci, B.; Petersson, G. A.; Nakatsuji, H.; Caricato, M.; Hratchian, X. L., Hratchian, H. P.; Izmaylov, A. F.; Bloino, J.; Zheng, G.; Sonnenberg, J. L.; Hada, M.; Ehara, M.; Toyota, K.; Fukuda, R.; Hasegawa, J.; Ishida, M.; Nakajima, T.; Honda, Y.; Kitao, O.; Nakai, H.; Vreven, T.; Montgomery, J. A., Jr.; Peralta, J. E.; Ogliaro, F.; Bearpark, M.; Heyd, J. J.; Brothers, E.; Kudin, K. N.; Staroverov, V. N.; Keith, T.; Kobayashi, R.; Normand, J.; Raghavachari, K.; Rendell, A.; Burant, J. C.; Iyengar, S. S.; Tomasi, J.; Cossi, M.; Rega, N.;



Millam, J. M.; Klene, M.; Knox, J. E.; Cross, J. B.; Bakken, V.; Adamo, C.; Jaramillo, J.; Millam, M. K., Knox, J. E.; Cross, J. B.; Bakken, V.; Adamo, C.; Jaramillo, J.; Gomperts, R.; Stratmann, R. E.; Yazyev, O.; Austin, A. J.; Cammi, R.; Pomelli, C.; Ochterski, J. W.; Martin, R. L.; Morokuma, K.; Zakrzewski, V. G.; Voth, G. A.; Salvador, P.; Dannenberg, J. J.; Dapprich, S.; Daniels, A. D.; Farkas, O.; Foresman, J. B.; Ortiz, J. V.; Cioslowski, J.; Fox, D. J. Gaussian16, Rev. B.01; Gaussian, Inc., Wallingford CT, **2016**.

25 Lee, C., Yang W., Parr, R. G., Development of the Colle-Salvetti correlation-energy formula into a functional of the electron density. *Phys. Rev. B.*, **1988**, 37, 785–789.

26 Perdew, J. P., Burke, K., Ernzerhof, M., Generalized Gradient Approximation Made Simple. *Phys. Rev. Lett.*, **1996**, 77, 3865–3868.

27 Pritchard, B.P., Altarawy, D., Didier, B., Gibson T. D., Windus, T. L. New Basis Set Exchange: An Open, Up-to-Date Resource for the Molecular Sciences Community. *J. Chem. Inf. Model.*, **2019**, 59, 4814–4820.

28 (a) London, F. J. Théorie quantique des courants interatomiques dans les combinaisons aromatiques. *J. Phys. Radium.*, **1937**, 8, 397–409; (b) Ditchfield, R. Self-consistent perturbation theory of diamagnetism: I. A gauge-invariant LCAO method for N.M.R. chemical shifts. *Mol. Phys.* **1974**, 27, 789–807; (c) Wolinski, K.; Hinton, J. F.; Pulay, P. Efficient Implementation of the Gauge-Independent Atomic Orbital Method for NMR Chemical Shift Calculations. *J. Am. Chem. Soc.* **1990**, 112, 8251–8260.

29 Wiberg, K., Application of the pople-santry-segal CNDO method to the cyclopropylcarbinyl and cyclobutylcation and to bicyclobutane. *Tetrahedron* **1968**, 24, 1083–1096.

30 NBO Program 6.0, Glendening, E. D.; Badenhop, J. K.; Reed, A. E.; Carpenter, J. E.; Bohmann, J. A.; Morales, C. M.; Landis, C. R.; Weinhold, F. Theoretical Chemistry Institute, University of Wisconsin, Madison, WI, **2013**.

31 Chemcraft-Graphical Software for Visualization of Quantum Chemistry Computations. Available online: <https://www.chemcraftprog.com> (accessed on 1 December 2021).

32 Lu, T.; Chen, F. Multiwfn: A multifunctional wavefunction analyzer. *J. Comput. Chem.* **2012**, *33*, 580–592.

## For Table of Contents Only

### Doubly Base-Stabilised Diborane(4) and Borato-Boronium Species and Their Chemistry with Chalcogens

Asif Ahmad,<sup>1</sup> Sourav Gayen,<sup>1</sup> Shivankan Mishra,<sup>1</sup> Zeenat Afsan,<sup>1</sup> Sébastien Bontemps,<sup>2</sup> and Sundargopal Ghosh\*<sup>1</sup>

An efficient, un-catalyzed method has been established for the synthesis of doubly-base stabilized diborane(4) and borato-boronium species using 2-mercaptopyridine and  $[\text{BH}_3 \cdot \text{THF}]$  (see picture).

